

24. K. M. Orcutt *et al.*, *Deep-Sea Res. II* **48**, 1583 (2001).  
 25. J. J. McCarthy, E. J. Carpenter, *J. Phycol.* **15**, 75 (1979).  
 26. T. Tyrrell *et al.*, *J. Plankton Res.* **25**, 405 (2003).  
 27. E. J. Carpenter, C. C. Price, *Science* **191**, 1278 (1976).  
 28. E. J. Carpenter, J. J. McCarthy, *Limnol. Oceanogr.* **20**, 389 (1975).  
 29. A. F. Post *et al.*, *Mar. Ecol. Prog. Ser.* **239**, 241 (2002).  
 30. R. R. Hood, A. Subramaniam, L. R. May, E. J. Carpenter, D. G. Capone, *Deep-Sea Res. II* **49**, 123 (2002).  
 31. We thank the officers and crew of the R/V *Knorr* for their outstanding support during the transatlantic VPR sampling. B. Walden provided facilities support for use of the VPR. F. Thwaites, A. Girard, and M. Alberico assisted in system deployment and operations. V. Kosyrev provided

daily altimetry maps and eddy positions to the ship based on data streams provided by R. Leben. J. Hummon processed the ship's acoustic Doppler current profiler data. We thank D. Capone, E. Carpenter, J. Waterbury, P. Falkowski, S. Dyhrman, E. Webb, and two anonymous reviewers for their helpful comments on this paper. Funding for development of the VPR was provided by a NSF Ocean Technology and Interdisciplinary Coordination grant OCE-9820099. Further support for VPR testing and operations was provided by NSF Oceanographic Technical Services grant OCE-0308366 and from the J. Seward Johnson Endowment Fund, the Penzance Foundation, and WHOI Biology Department Discretionary Funds. C.S.D. was supported by the Richard B. Sellars Endowed Research

Fund, the Andrew W. Mellon Foundation Endowed Fund for Innovative Research, and a fellowship from WHOI's Ocean Life Institute. D.J.M. was supported by NSF grant OCE-0241310 and NASA grant NNG04GR22G.

#### Supporting Online Material

[www.sciencemag.org/cgi/content/full/312/5779/1517/DC1](http://www.sciencemag.org/cgi/content/full/312/5779/1517/DC1)  
 Materials and Methods  
 Figs. S1 to S3  
 Table S1  
 References and Notes

7 December 2005; accepted 13 April 2006  
 10.1126/science.1123570

## TOPLESS Regulates Apical Embryonic Fate in *Arabidopsis*

Jeff A. Long,<sup>1\*</sup> Carolyn Ohno,<sup>2</sup> Zachery R. Smith,<sup>1</sup> Elliot M. Meyerowitz<sup>2</sup>

The embryos of seed plants develop with an apical shoot pole and a basal root pole. In *Arabidopsis*, the *topless-1* (*tpl-1*) mutation transforms the shoot pole into a second root pole. Here, we show that TPL resembles known transcriptional corepressors and that *tpl-1* acts as a dominant negative mutation for multiple TPL-related proteins. Mutations in the putative coactivator *HISTONE ACETYLTRANSFERASE GNAT SUPERFAMILY1* suppress the *tpl-1* phenotype. Mutations in *HISTONE DEACETYLASE19*, a putative corepressor, increase the penetrance of *tpl-1* and display similar apical defects. These data point to a transcriptional repression mechanism that prevents root formation in the shoot pole during *Arabidopsis* embryogenesis.

The apical/basal axis of *Arabidopsis* embryos is established during the first cell division of the zygote, and auxin accumulation and response have been shown to be important for early steps in axis establishment (1–5). As the embryo matures, specific cell types become apparent, and a clear shoot/root axis is visible at the transition stage of development (6, 7). Although several mutants have been isolated that affect the formation of specific patterning elements of the shoot at the transition stage of embryogenesis, only *topless-1* (*tpl-1*) so far switches the identity of the shoot into that of a root (8–11). It is therefore likely that TPL is acting at a different level of control than those factors that have previously been isolated.

*tpl-1* mutants are temperature sensitive and at the restrictive temperature (29°C) transform the embryonic shoot pole into a second root pole that gives rise to a double-root seedling (11) (Fig. 1, A and B). At lower temperatures, *tpl-1* embryos fail to form a shoot apical meristem and show varying degrees of cotyledon fusion (Fig. 1, C to E). We view these phenotypes as a result of partial apical-to-basal transformation during embryogenesis (11) (fig. S1). Previous work has shown that transition-stage *tpl-1* embryos lack or have reduced expression of genes associated with the apical half of the embryo, whereas the

expression patterns of genes associated with the basal half of the embryo are expanded into the apical half and are ultimately duplicated. Pre-transition stage *tpl-1* embryos are morphologically indistinguishable from those of the wild type.

To examine the molecular organization of the apical half of *tpl-1* pre-transition stage embryos, we performed *in situ* hybridizations with the

transcription factor *WUSCHEL* (*WUS*) (10). *WUS* is initially expressed in a small group of cells in the apical half of 16-cell-stage embryos. *WUS* mRNA accumulated normally in *tpl-1* globular-stage embryos, but was absent in transition-stage embryos at 29°C (Fig. 1, F to H). This indicates that early *tpl-1* embryos have established an apical axis with the correct organization, but this fate is lost or masked at the transition stage.

*tpl-1* was mapped to bacterial artificial chromosome F7H2 on chromosome 1 using polymerase chain reaction-based markers (11). We found two base-pair substitutions in At1g15750 (12) that cosegregated with the *tpl-1* phenotype and result in a change of a lysine (K) to a methionine (M) at amino acid 92 and an asparagine (N) to a histidine (H) at amino acid 176 of the predicted protein (13). Concurrently, we conducted a high-temperature ethylmethane sulfonate suppressor screen in the *tpl-1* background and found five semidominant suppressors that mapped to the original TPL locus. We sequenced At1g15750 from these lines and found that each harbored a second site mutation that is

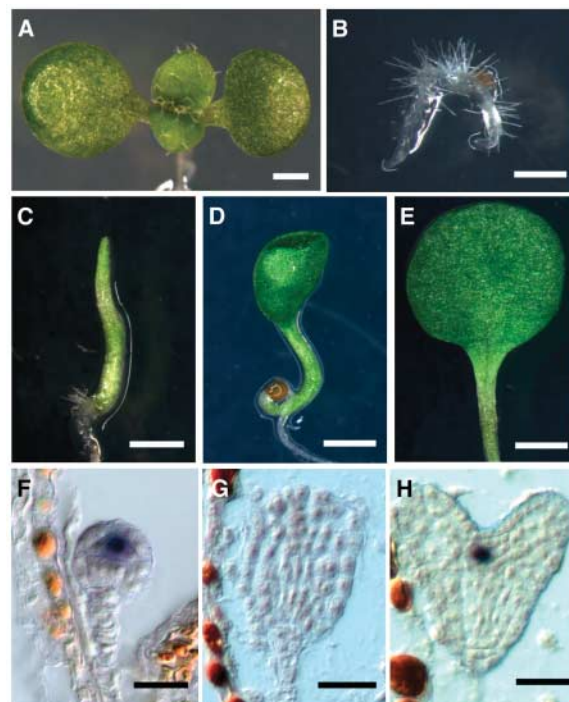


**Fig. 1.** Effects of *topless-1* on embryonic polarity. (A) Wild-type 5-day-old seedling. (B) A *tpl-1* double-root seedling. (C) A *tpl-1* pin seedling lacking cotyledons. (D) A *tpl-1* tube seedling. (E) A *tpl-1* monocot seedling with two fused cotyledons. (F) *WUS* mRNA accumulation in a *tpl-1* globular-stage embryo grown at 29°C. (G) *WUS* mRNA does not accumulate in a *tpl-1* heart-stage embryo. (H) Wild-type heart-stage embryo accumulating *WUS* mRNA in a small group of cells in the developing meristem. Scale bars: 1 mm (A to E), 25  $\mu$ m (F to H).

<sup>1</sup>Plant Biology Laboratory, The Salk Institute for Biological Sciences, 10010 North Torrey Pines Road, La Jolla, CA 92037, USA. <sup>2</sup>Division of Biology, California Institute of Technology, 1200 East California Boulevard, Pasadena, CA 91125, USA.

\*To whom correspondence should be addressed. E-mail: long@salk.edu

predicted to reduce or abolish gene function (Fig. 2A). That second site mutations in the *tpl-1* mutant gene suppress the *tpl-1* phenotype indicates that *tpl-1* is a gain-of-function allele. The semidominant nature of these loss-of-function alleles also implies a dosage requirement for the *tpl-1* protein.

*TPL* is predicted to encode an 1131-amino acid protein containing 11 WD40 repeats at the C terminus (Fig. 2A). At the N terminus, TPL has predicted lissencephaly type 1–like homology (LisH) and C-terminal to LisH (CTLH) domains that are thought to be important either for self-dimerization or for other protein-protein interactions (14). TPL also contains a 100-amino acid region rich in prolines (24 out of 100 amino acids). A similar domain organization is found in the TUP1/GROUCHO and LEUNIG family of transcriptional corepressors, although there is little sequence identity between TPL and these proteins (15, 16). Four other predicted proteins in *Arabidopsis* share extensive amino acid similarity with TPL and have been named TOPLESS-RELATED (TPR) (fig. S2).

In situ hybridization experiments revealed that *TPL* mRNA accumulates in all cells of the embryo as well as in extra-embryonic tissues (Fig. 2, B and C). *TPL* mRNA accumulates to higher levels in the embryo proper during early embryogenesis and in the developing vasculature in later stages. A TPL-GREEN FLUORESCENT PROTEIN (GFP) translational fusion under the control of 4.1 kb of upstream genomic sequences rescued the *tpl-1* phenotype when homozygous and localized to the nuclei of all cells in transgenic plants (Fig. 2D). This again indicates a dosage dependence for the *tpl-1* protein and suggests that the wild-type version of the protein can outcompete the mutant form.

To determine if both of the amino acid changes found in the original *tpl-1* allele were

necessary for the *tpl-1* phenotype, we transformed a *tpl* transfer DNA (T-DNA) insertion line (*tpl-8*) with TPL-GFP fusion proteins containing either both mutations (*tpl-1*), only the K92M mutation, or only the N176H mutation (17). The *tpl-1* phenotype was observed in plants carrying either the *tpl-1* transgene or the N176H transgene (16 and 15 lines, respectively). However, we did not observe any *tpl* phenotypes in 29 independent lines transformed with the K92M construct despite nuclear GFP accumulation comparable to that of lines with a *tpl-1* phenotype. Therefore, the N176H mutation is necessary and sufficient to cause the *tpl-1* phenotype.

*tpl* loss-of-function alleles display no obvious phenotype when grown at the restrictive temperature (Fig. 2E). We therefore hypothesized that TPL may act redundantly with the other TPR proteins. We generated *tpl-2*; *tpl-1*; *tpl-3*; *tpl-4* quadruple mutant lines and transformed them with a *TPR2* RNA interference (RNAi) transgene. We obtained five stable transgenic lines that displayed the original *tpl-1* phenotypes (Fig. 2F). This indicates that *tpl-1* acts as a type of dominant negative allele for multiple *TPR* family members.

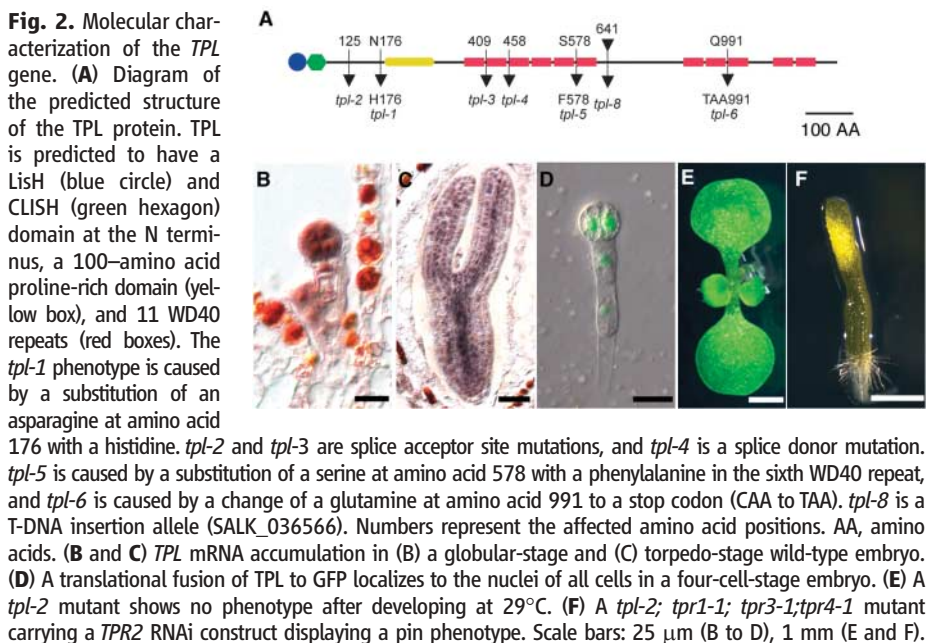
In the high-temperature suppressor screen, we also isolated two alleles of a recessive extragenic suppressor of *tpl-1* designated *big top* (*bgt*). At 24°C, the progeny of plants homozygous for *tpl-1* and heterozygous for *bgt-1* segregated 24.1% wild-type seedlings (Fig. 3B) ( $n = 513$ ). This same combination with *bgt-2* yielded 19.3% wild-type seedlings ( $n = 1746$ ). We therefore characterized *bgt-1* in more detail. Morphologically, *tpl-1*; *bgt-1* embryos form cotyledons at the transition stage of embryogenesis, although they appear slightly stunted at later stages as compared to wild-type embryos (Fig. 3, C and D). To examine the apical pattern

of *tpl-1*; *bgt-1* embryos, we examined the expression of *WUS* in these double mutants at 29°C. At all stages tested, *tpl-1*; *bgt-1* embryos maintained the expression of *WUS* in the appropriate number of cells, indicating that the top half of these embryos had not lost their apical identity (Fig. 3, E to G).

We mapped the *bgt-1* mutation and found that it was tightly linked to marker TSA1 on chromosome 2 (0 recombinants out of 606 chromosomes). This genomic region contains the *Arabidopsis* homolog of the histone acetyltransferase GCN5 (*HAG1*) (also known as *atGCN5*) (18, 19). In other eukaryotes, GCN5 is recruited to specific promoters by DNA binding transcription factors and is thought to promote transcription by acetylating the N-terminal tail of histone H3 (20). Sequencing revealed that both *bgt-1* and *bgt-2* carried lesions in *HAG1* (Fig. 3A). We therefore renamed these alleles *hag1-3* and *hag1-4*. T-DNA insertions in the tenth intron (*hag1-5*) and in the first intron (*hag1-6*) also suppressed *tpl-1* (Fig. 3A). All four *hag* alleles have no obvious embryonic phenotypes, although postembryonically they display pleiotropic phenotypes similar to that of a previously described allele (18). A translational fusion of a 4.3-kb *HAG1* genomic clone to GFP rescued the *hag1-3* mutant, and the protein was found in the nuclei of all cells examined (Fig. 3H). The observation that a mutation in a coactivator suppresses the *tpl-1* phenotype is consistent with TPL acting as a corepressor.

In eukaryotes, transcription from many promoters can be repressed through the activity of histone deacetylases. The RPD3 family of histone deacetylases can act as transcriptional corepressors, and in *Drosophila*, Groucho and an RPD3-like protein work together to specify anterior/posterior polarity (21). The *Arabidopsis* genome contains four class 1 RPD3-like proteins [Histone Deacetylase (HDA) 6, 7, 9, and 19] (22). In a screen for mutants that affect floral organ identity, a T-DNA allele of *HDA19* (*hda19-1*) (also known as *atHDI* and *RPD3a*) was isolated that displays floral phenotypes similar to those of *tpl-1* (23–25). A second T-DNA allele (*hda19-2*) was isolated from the Wisconsin *Arabidopsis* Knockout facility and found to show similar phenotypes (Fig. 4A). We therefore examined the role and expression of *HDA19* more closely during embryogenesis.

*HDA19*, like *TPL* and *HAG1*, is broadly expressed throughout embryogenesis, and a GFP fusion protein localizes to the nuclei of all embryonic cells (Fig. 4, B and C). Phenotypically, both *hda19-1* and *hda19-2* seedlings when grown at 24°C have narrow cotyledons as compared to those of the wild type (Fig. 4D). However, when mutants homozygous for either allele were grown at 29°C, mutant seedlings displayed several *tpl-1*-like phenotypes, including monocots, tubes, and pins, indicating that these *hda19* alleles are temperature sensitive (Fig. 4E). These phenotypes were seen in 32%



of *hda19-1* seedlings ( $n = 397$ ) and 28% of *hda19-2* seedlings ( $n = 330$ ). A morphological analysis of *hda19-1* embryos at 29°C showed that both the root and the shoot can be disorganized (Fig. 4F), indicating that HDA19 may play a broader role in embryogenesis than TPL.

We then examined the progeny of *hda19-1*<sup>-/-</sup>; *tpl-1*<sup>+/-</sup> plants grown at 24°C, a temperature at which *tpl-1* segregates as a recessive (11). We found that 45% of the resulting seedlings showed cotyledon fusion defects ( $n = 804$ ) instead of the expected 25%, indicating that

HDA19 may act on some of the same target genes as TPL during embryogenesis. In agreement with this hypothesis, we identified *tpl-1*; *hda19-1*; *hag1-3* triple-mutant seedlings from plants grown at 24°C, as well as 29°C, and found that they displayed two narrow cotyledons like the *hda19-1* single mutant (Fig. 4G). Therefore, *hag1-3* mutants can suppress *tpl-1* mutant phenotypes even in the absence of functional HDA19.

Recent work on embryonic polarity in *Arabidopsis* has focused on auxin transport and the first embryonic cell divisions in establishing the apical/basal axis (4, 26). Our studies have uncovered a set of proteins involved in a new step in axis formation, during the transition stage of embryogenesis, when shoot fate becomes fixed and distinct from root fate. We propose that at the transition stage of embryogenesis, TPL and other TPR proteins are necessary to repress the expression of root-promoting genes in the top half of the embryo to allow proper differentiation of the shoot pole. A histone deacetylase, HDA19, works in conjunction with TPL during this process, although it appears to have TPL-independent roles as well (27). HAG1 is necessary for the complete transformation of the apical half into a root, likely by activating the transcription of derepressed root-specific genes in the apical half of the embryo. However, HAG1 is dispensable for the formation of the basal “true” root. Conceptually, these two steps of polarity determination are similar to what has been reported in the brown alga *Fucus*, where axis formation and fixation are temporally distinct (28). In *Arabidopsis*, we propose that the axis formation step occurs during the first cell divisions of the embryo and likely relies on polar auxin distribution (4). Only later, at the transition stage of embryogenesis, does the axis become fixed, at which time the plant requires a chromatin-mediated transcriptional repression system for axis stabilization.

**Fig. 3.** Characterization of *hag1* alleles and genetic interactions with *tpl-1*. (A) Diagram of the predicted structure of HAG1 that contains a conserved histone acetyltransferase domain (red box) and a bromo domain (yellow box). *hag1-3* contains a stop codon at amino acid 478 (TGG to TGA); *hag1-4* contains a splice donor mutation at amino acid 389; *hag1-5* is a T-DNA insertion in the 10th intron (SALK\_048427); and *hag1-6* is a T-DNA insertion in the first intron (SALK\_150784). (B) A *tpl-1*;*hag1-3* double-mutant seedling grown at 24°C. (C and D) Cleared torpedo-stage embryos of (C) *tpl-1*;*hag1-3* and (D) wild-type seedling grown at 29°C. (E to G) WUS mRNA accumulation in (E) *tpl-1*, (F) *tpl-1*;*hag1-3*, and (G) wild-type 29°C grown torpedo-stage embryos. (H) A HAG1-GFP fusion protein localizes to the nuclei of all cells of a 16-cell-stage embryo. Scale bars: 1 mm (B), 25 μm (C to H).

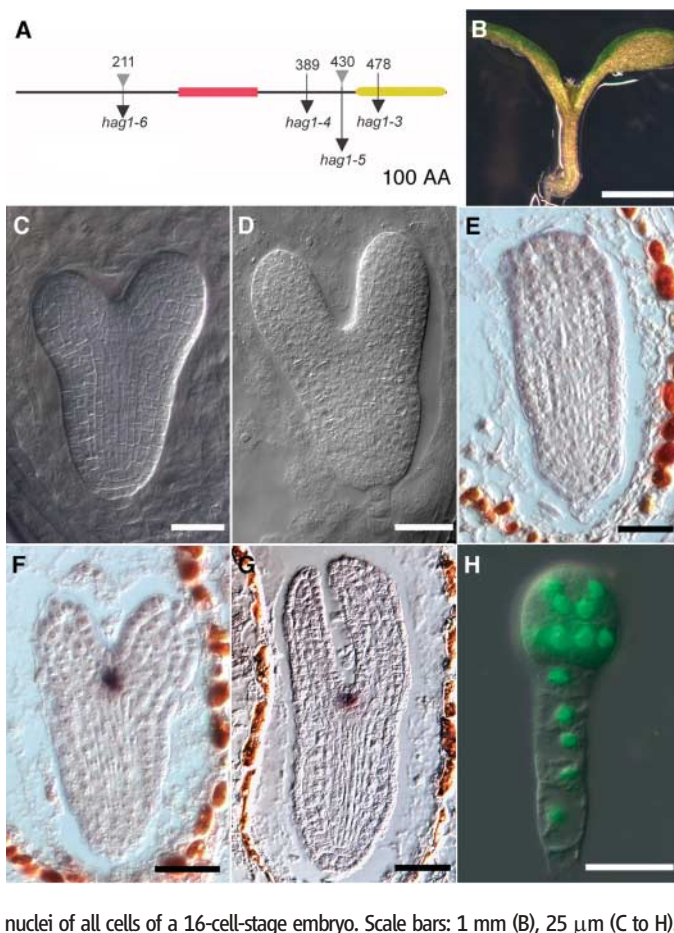
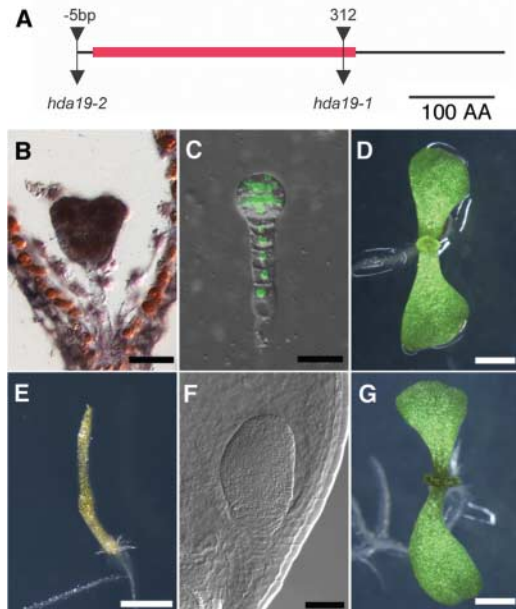


**Fig. 4.** Characterization and genetic interactions of HDA19. (A) Predicted structure of HDA19. *hda19-1* contains a T-DNA insertion that disrupts amino acid 312 in the histone deacetylase domain (red box). *hda19-2* contains a T-DNA insertion 5 base pairs upstream of the start codon. (B) mRNA accumulation of HDA19 in all cells of an early heart-stage embryo. (C) A HDA19-GFP fusion protein localizes to the nuclei of all cells of a 16-cell-stage embryo. (D) Seedling phenotype of *hda19-1* when grown at 24°C. (E) A *hda19-2* seedling displaying a pin phenotype when grown at 29°C. (F) A *hda19-1* heart-stage embryo grown at 29°C showing both shoot and root defects. (G) A *tpl-1*;*hag1-3*;*hda19-1* triple-mutant seedling grown at 24°C. Scale bars: 25 μm (B, C, and F), 1 mm (D, E, and G).



**References and Notes**

1. I. Bblilou *et al.*, *Nature* **433**, 39 (2005).
2. S. G. Mansfield, L. G. Briarty, *Can. J. Bot.* **69**, 461 (1991).
3. T. Steinmann *et al.*, *Science* **286**, 316 (1999).
4. J. Friml *et al.*, *Nature* **426**, 147 (2003).
5. C. S. Hardtke, T. Berleth, *EMBO J.* **17**, 1405 (1998).
6. J. A. Long, M. K. Barton, *Development* **125**, 3027 (1998).
7. A. Haecker *et al.*, *Development* **131**, 657 (2004).
8. M. Aida, T. Ishida, M. Tasaka, *Development* **126**, 1563 (1999).
9. M. K. Barton, R. S. Poethig, *Development* **119**, 823 (1993).
10. T. Laux, K. F. Mayer, J. Berger, G. Jurgens, *Development* **122**, 87 (1996).
11. J. A. Long, S. Woody, S. Poethig, E. M. Meyerowitz, M. K. Barton, *Development* **129**, 2797 (2002).
12. This protein was recently reported to interact with WUS in a two-hybrid screen (29).
13. Materials and methods are available as supporting material on Science Online.
14. R. D. Emes, C. P. Ponting, *Hum. Mol. Genet.* **10**, 2813 (2001).
15. G. Chen, A. J. Courey, *Gene* **249**, 1 (2000).
16. J. Conner, Z. Liu, *Proc. Natl. Acad. Sci. U.S.A.* **97**, 12902 (2000).

17. J. M. Alonso *et al.*, *Science* **301**, 653 (2003).  
 18. K. E. Vlachoniasos, M. F. Thomashow, S. J. Triezenberg, *Plant Cell* **15**, 626 (2003).  
 19. C. Bertrand, C. Bergounioux, S. Domenichini, M. Delarue, D. X. Zhou, *J. Biol. Chem.* **278**, 28246 (2003).  
 20. M. H. Kuo *et al.*, *Nature* **383**, 269 (1996).  
 21. G. Chen, J. Fernandez, S. Mische, A. J. Courey, *Genes Dev.* **13**, 2218 (1999).  
 22. R. Pandey *et al.*, *Nucleic Acids Res.* **30**, 5036 (2002).  
 23. C. Ohno, E. M. Meyerowitz, personal communication.  
 24. K. Wu, L. Tian, K. Malik, D. Brown, B. Miki, *Plant J.* **22**, 19 (2000).
25. L. Tian, Z. J. Chen, *Proc. Natl. Acad. Sci. U.S.A.* **98**, 200 (2001).  
 26. T. Hamann, E. Benkova, I. Baurle, M. Kientz, G. Jurgens, *Genes Dev.* **16**, 1610 (2002).  
 27. C. Zhou, L. Zhang, J. Duan, B. Miki, K. Wu, *Plant Cell* **17**, 1196 (2005).  
 28. B. Goodner, R. S. Quatrano, *Plant Cell* **5**, 1471 (1993).  
 29. M. Kieffer *et al.*, *Plant Cell* **18**, 560 (2006).  
 30. We thank L. Jones, J. Nemhauser, and F. Wellmer for critical reading of the manuscript. We also thank M. Hannon and K. Shively for assistance with the *tpl* loss-of-function alleles and D. B. Vert and N. Geldner for

technical assistance. This work was supported by a Helen Hay Whitney postdoctoral fellowship and by NIH grants GM072764 (to J.A.L.) and GM45697 (to E.M.M.).

### Supporting Online Material

www.sciencemag.org/cgi/content/full/312/5779/1520/DC1  
 Materials and Methods  
 Figs. S1 and S2  
 References

14 December 2005; accepted 27 April 2006  
 10.1126/science.1123841

# Tim50 Maintains the Permeability Barrier of the Mitochondrial Inner Membrane

Michael Meinecke,<sup>1</sup> Richard Wagner,<sup>1\*</sup> Peter Kovermann,<sup>1†</sup> Bernard Guiard,<sup>2</sup> David U. Mick,<sup>3</sup> Dana P. Hutu,<sup>3,4</sup> Wolfgang Voos,<sup>3</sup> Kaye N. Truscott,<sup>3,5</sup> Agnieszka Chacinska,<sup>3</sup> Nikolaus Pfanner,<sup>3\*</sup> Peter Rehling<sup>3</sup>

Transport of metabolites across the mitochondrial inner membrane is highly selective, thereby maintaining the electrochemical proton gradient that functions as the main driving force for cellular adenosine triphosphate synthesis. Mitochondria import many preproteins via the presequence translocase of the inner membrane. However, the reconstituted Tim23 protein constitutes a pore remaining mainly in its open form, a state that would be deleterious in organello. We found that the intermembrane space domain of Tim50 induced the Tim23 channel to close. Presequences overcame this effect and activated the channel for translocation. Thus, the hydrophilic cis domain of Tim50 maintains the permeability barrier of mitochondria by closing the translocation pore in a presequence-regulated manner.

Most mitochondrial proteins are synthesized as preproteins in the cytosol and must be imported across outer and inner mitochondrial membranes (1–6). The mitochondrial inner membrane generates and maintains a proton-motive force that is crucial to drive the  $F_0F_1$ -ATP synthase, which is the major machine for cellular adenosine triphosphate (ATP) synthesis (7, 8). How can the permeability barrier of the inner membrane for small ions such as protons be maintained while large hydrophilic channels for the passage of polypeptide chains exist?

The presequence translocase of the inner membrane (TIM23 complex) translocates hundreds of different preproteins into the matrix. The TIM23 complex contains the

pore-forming protein Tim23 and three additional membrane proteins, Tim17, Tim21, and Tim50. Tim23 consists of a membrane-embedded domain, containing the large translocation channel, and a domain in the intermembrane space (IMS) that recognizes the N-terminal presequences of preproteins (4, 6, 9–12). Tim50 and Tim21 each consist of a single transmembrane segment and a large IMS domain, which interact with preproteins and with the translocase of the outer membrane, respectively (13–17). Tim17 is largely embedded in the inner membrane and promotes cooperation of the presequence translocase with the associated import motor (PAM complex) (13). PAM is a multisubunit machinery on the matrix side of the inner membrane with the matrix heat shock protein 70 (Hsc70) (Ssc1) as the central ATP-consuming subunit. How the presequence channel is regulated to permit translocation of preproteins but prevent leakage of small ions is unknown.

To understand the regulation of the Tim23 channel, we took a combinatorial *in vitro* and *in organello* approach. When purified Tim23 was reconstituted into liposomes and subjected to electrophysiological analysis in a planar lipid bilayer system, a cation-permeating channel with the reported characteristics of the presequence channel of the mitochondrial inner membrane was observed;

however, the pore remained mainly in an open state (Fig. 1A) (3, 10). The Tim23 channel did not display an intrinsic activity that forced fast channel closure. In organello, an open 450-pS channel, present in about 300 copies per isolated mitochondrion (18, 19), would seriously compromise the permeability barrier and the bioenergetic activity of the inner membrane. We thus asked whether additional components associated with Tim23 might play a role in regulating channel closure by comparing the membrane potential ( $\Delta\psi$ ) of yeast mutant mitochondria.

The presequence translocase exists in two forms. One form (TIM23<sup>SOFT</sup>) contains Tim23, Tim17, Tim50, and Tim21 and can direct preproteins into the inner membrane. The second form transports preproteins into the mitochondrial matrix and is associated with the motor PAM but lacks Tim21 (fig. S1A) (13, 20). We assessed the  $\Delta\psi$  values of mitochondria isolated from different *tim* and *pam* mutants with the use of the potential-sensitive fluorescent dye 3,3'-dipropylthiadicarbocyanine iodide [DiSC<sub>3</sub>(5)] (21) (Fig. 1, B to D). *tim17* and *tim21* mutant mitochondria displayed  $\Delta\psi$  values comparable to that of wild-type mitochondria (13), whereas *tim50* mutant mitochondria (14) showed a severe reduction of  $\Delta\psi$  (Fig. 1, B and D). In the translocon of the endoplasmic reticulum, the luminal Hsp70 (BiP) and a DnaJ protein are involved in regulation of the Sec61 channel (22, 23). Because PAM contains the Hsp70 Ssc1 and an associated DnaJ protein (Pam18), we asked whether the  $\Delta\psi$  across the inner membrane was affected in mitochondria containing mutant versions of PAM subunits. However, neither *ssc1*, nor *pam18*, nor *tim44* mutant mitochondria (21, 24–28) exhibited a significant reduction in  $\Delta\psi$  relative to wild-type mitochondria (Fig. 1, C and D), consistent with the observation that only two components, Tim50 and Tim17, are associated with Tim23 in both forms of the presequence translocase (13). Because the Tim23 channel is active in both forms, a factor that regulates channel closure should be present in either form. We conclude that functional Tim50 is required to maintain the  $\Delta\psi$  in intact mitochondria.

The IMS domain of Tim50 interacts with the IMS domain of Tim23 (14–16). [Tim50 does

<sup>1</sup>Biophysik, Universität Osnabrück, FB Biologie/Chemie, D-49034 Osnabrück, Germany. <sup>2</sup>Centre de Génétique Moléculaire, Laboratoire propre du CNRS, F-91190 Gif-sur-Yvette, France. <sup>3</sup>Institut für Biochemie und Molekularbiologie, Universität Freiburg, Hermann-Herder-Straße 7, D-79104 Freiburg, Germany. <sup>4</sup>Fakultät für Biologie, Universität Freiburg, Schänzlestraße 1, D-79104 Freiburg, Germany. <sup>5</sup>Department of Biochemistry, La Trobe University, Melbourne 3086, Australia.

\*To whom correspondence should be addressed. E-mail: wagner@biologie.uni-osnabrueck.de (R.W.); nikolaus.pfanner@biochemie.uni-freiburg.de (N.P.)

†Present address: Institute for Plant Biology, Molecular Physiology, University of Zürich, 8008 Zürich, Switzerland.